

Article

Influence of Impurities in Electrical Contacts on Increasing the Efficiency of Energy Transmission

Dušan Medved' * , Ľubomír Beňa , Michal Kolcun and Marek Pavlík 

Department of Electric Power Engineering, Faculty of Electrical Engineering and Informatics, Technical University of Košice, Letná 9, 042 00 Kosice, Slovakia; lubomir.bena@tuke.sk (Ľ.B.); michal.kolcun@tuke.sk (M.K.); marek.pavlik@tuke.sk (M.P.)

* Correspondence: dusan.medved@tuke.sk; Tel.: +421-55-602-3555

Abstract: The aim of this paper is to analyze the heat distribution in the high-current electrical contact under the action of an assumed current of 3000 A using mathematical modeling and simulation. Electrical contacts that carry high currents are an essential component of many electric devices. In transmission and distribution systems, the electrical contacts are of particular importance because they must withstand adverse weather conditions that decrease their effectiveness. Therefore, it is essential to detect any rise in temperature of the electrical contact to ensure efficient and reliable energy transmission. For this paper, simulations of the temperature field in direct electrical contact were carried out in ANSYS and discussed. During the simulation, a high-current electric contact was exposed to 3000 A current and the change of the adverse effects of contaminated contact layers affected temperature field. According to the results, electric contact in good condition (represented by impurity layer of lower resistivity) had a temperature of 80 °C lower than an electric contact that was worn out (represented by impurity layer of higher resistivity). The investigation of the resistivity of contaminated contact layers has led to the determination of permissible values for the power grid operators to maintain these types of devices when temperatures rise.

Keywords: electrical contact; simulation; ANSYS; temperature field; high current



Citation: Medved', D.; Beňa, Ľ.; Kolcun, M.; Pavlík, M. Influence of Impurities in Electrical Contacts on Increasing the Efficiency of Energy Transmission. *Energies* **2022**, *15*, 2339. <https://doi.org/10.3390/en15072339>

Academic Editors: Andrea Mariscotti and King Jet Tseng

Received: 30 November 2021

Accepted: 21 March 2022

Published: 23 March 2022

Publisher's Note: MDPI stays neutral with regard to jurisdictional claims in published maps and institutional affiliations.



Copyright: © 2022 by the authors. Licensee MDPI, Basel, Switzerland. This article is an open access article distributed under the terms and conditions of the Creative Commons Attribution (CC BY) license (<https://creativecommons.org/licenses/by/4.0/>).

1. Introduction

Electrical contact is the point of contact of two objects through which an electric current passes, one of the objects is mostly movable and the other fixed [1]. However, the junction of the contacts does not take place over their entire surface, but only in a few small areas, so that the passage of current is limited and manifests itself as a transient resistance of the contacts [2].

1.1. Related Works

In electrical systems, electrical contacts play a simple but crucial role [3,4]. Gatzsche, M., et al. verified the voltage-temperature relation of high-current applications [5]. They investigated V-T relation dependence with a high current experiment for steady-state continuous operation and numerical calculations for transient short-time operation. Behrens, V., et al. describe the effect of ambient temperature and contact force on contact resistance and the consequent overheating behavior of electric power contacts [6]. Israel T., et al. devoted work to high-current impact of short circuits on contact elements in specific types of power electric contacts. Their investigation was supported by the FEA simulation [7]. The common attribute of these works is, that the electrical contacts provide an interface between circuit segments, to connect and disconnect segments as needed through electric contacts. While this may seem straightforward at first glance, the design of this type of connection (electric contact) requires careful planning and consideration of all possible adverse effects [3,8]. When a component of a system is designed improperly, excessive discoloration, welding wear, mechanical damage,

and corrosion wear can occur, resulting in incorrect connections [9,10]. In order to minimize the occurrence of these fault modes, the contacts must maintain low contact resistance, minimal electrical noise, and reliable connection and disconnection capabilities.

Electric arcs create a tan on most of the contacts during tripping when the circuit is interrupted by an electrical fault [11–13]. The most fault-prone components of devices and circuits are contacts, so they are made with special materials. Hundreds of different materials are available and they are successfully employed for many different purposes [14,15].

Considering the above factors, it is necessary to determine the thermal behavior of the electrical contacts. Practical measurements can be difficult, so numerical calculations are required. The temperature field distribution can be calculated with finite element analysis software that can be used for these calculations. Saha, S., et al., determined the electro-thermo-mechanical contact analysis of high-current electric contact during the change of material properties [16]. Monnier, A., et al., realized simulation of specific sphere-plane electrical contact where they considered mechanical, electrical, thermal coupled-field simulation [17]. The high current flow path simulation was investigated by Szulborski, M., et al [18]. They utilized the FEA simulation for the transient thermal analysis of the circuit breaker current path and investigated the overheating of the contacts.

1.2. Paper Contributions

The purpose of this paper is to present the results of analysis of the influence of impurities on high-current contacts on temperature field distribution. To assess multiple scenarios, we used the ANSYS simulation software. Based on the best and worse scenarios, it was found that surface impurities (characterized by changed resistivity) led to overheating of the electric contact joint. Graphs and numerical results were presented. This paper's major goal, and the novel contribution, is to examine the influence of surface resistivity on the overall temperature field of the high-current contact. Section 2 contains the description of the main control properties of electro-technical materials used for electrical contacts. Section 3 presents the thermal analysis of electrical contacts. In Section 4, there is presented and discussed influence of materials and impurities of direct contact on temperature distribution. The main conclusions are discussed in Section 5.

2. Control of Properties of Electro-Technical Materials for Electrical Contacts

For the best function of the devices, it is necessary to ensure the smallest possible contact resistance between the contacts. This depends on the contact force of the contacts, the type of junction of the contacts and the foreign layers. The resistance of the contacts at higher contact forces (according to Babikow) is given by the formula (for contact pressing force F between 10 and 200 N) [19]:

$$R_k = k \cdot F^{-n} [\Omega], \quad (1)$$

where k is the type of material used and the effect of foreign layers (material dependent proportionality factor), F is the pressing force and n is the type of contact (shape dependent exponent of the contact force). The pressing force is provided by various mechanisms, springs or the structural arrangement of the contacts (S-contact, knife contact, etc.). Typical values of material dependent proportionality factor k and shape dependent exponent of the contact force n are presented in Tables 1 and 2.

Table 1. Table of material dependent proportionality factor k [19].

Material Combination	k
Copper—copper	$(0.08 \div 0.14) \times 10^{-3}$
Aluminum—aluminum	$(3 \div 6.7) \times 10^{-3}$
Brass—brass	0.67×10^{-3}
Steel—silver	0.06×10^{-3}
Steel—copper	3.1×10^{-3}
Steel—brass	3×10^{-3}

Table 2. Table of shape dependent exponent of the contact force n [19].

Contact Shape	n
Flat—flat	1
Pyramid—flat	0.5
Sphere—flat	0.6
Sphere—sphere	0.5
Multi-strand brush—flat	1
Current bar (busbar) contact	$0.5 \div 0.7$

The reduction of contact resistance begins with the selection of the correct electrical contact material, regular inspection, replacement of worn contacts, cleaning and maintenance of corroded electrical contacts. Low roughness tends to increase the number of spots, and thus to reduce the contact resistance. Operators must clean electrical contacts regularly to reduce their contact resistance and ensure good operational safety and performance [20,21].

Electro-technical materials occur in different operating conditions. With the development of technology, the requirements for the complexity of these conditions also increase. Therefore, until now, the sufficient properties of the electro-technical material may no longer be suitable in demanding conditions. The properties of such materials need to be modified or the material replaced. For example, copper shows a distinctive mechanical stress loss of an elasticity behavior [22,23]. The compensation associated with the development of a completely new material is not easy and is costly. A simpler and more efficient way is to adjust the properties of a given material to suit the required conditions. Intentional modification of material properties is called property management. There are two methods of controlling the properties of materials, namely control of properties by *changing the structure* and control of properties by changing the composition [15].

Overheating of the Current Path of the Electrical Contact

Overheating of the current path is an important parameter that must be closely monitored in electrical equipment. This parameter is closely related to the operating condition, reliability, safety and service life of the electrical equipment [24]. When designing and operating multiple devices, this parameter is a limiting factor. Temperatures higher than operating temperatures lead to degradation of the conductor insulation, which in turn causes fault conditions.

The basic factors for the heating of the current path are the current load and the electrical resistance of the conductor from which the heating originates. Other parameters include the degree and method of cooling the conductor, where there are several ways of heat transfer. Less important parameters are the operating conditions, the ambient temperature, the quality of the contacts, the speed, the wind direction and the heating caused by solar radiation or the thermal conductivity of the conductors and insulating materials [25]. Overheating can be observed also in the case of two different materials are used, for example copper and aluminum. In the circuit consisting of dissimilar conductors, there could be occurred a thermoelectric power, and the contact is maintained at different temperatures. We can use the Seebeck effect, to monitor the particular place of electrical contact to detect overheating [26]. In addition, overheating can occur during some physical

events, such as the skin effect or the influence of the proximity of conductors, which affect the overall resistance of the conductor.

The passage of electric current through the conductor causes losses, which are manifested by overheating of the current path. Part of this heat is stored in the conductor depending on the temperature of the material and the rest is dissipated to the surroundings. In the steady-state operating state with constant heating, when the temperature of the conductor is constant, the entire part of the generated heat is dissipated to the surroundings. In the case of transients in which the value of the electric current is not constant, it is necessary to take into account the actual thermal capacity of the conductor, or the thermal capacity of all components of the thermal analysis. When constructing a model of current path overheating, it's crucial to analyze what's going on in each scenario and what can be neglected. A specific event must be described by an equation that takes into account its size and course of action. For a general description of the effect, this equation is [24,27]:

$$P_z = c \cdot V \cdot \frac{d\vartheta}{dt} + P_0 \text{ [W]} \quad (2)$$

where P_z is the heating power [W], c is the specific volume heat capacity of the conductor [$\text{J}/(\text{m}^3 \cdot ^\circ\text{C})$], V is the volume of the conductor [m^3], ϑ is the instantaneous temperature of the conductor [$^\circ\text{C}$] and P_0 is the cooling capacity [W].

3. An Analysis of the Thermal Characteristics of Electrical Contacts

As we examine the effect of electric current on the temperature of selected contacts in this chapter, we consider that the individual contacts might overheat when the electric current passes through them, resulting in contact degradation or failure of equipment. To achieve the best results, the dimensions of the contact and the contact material require careful consideration when designing the contact. In addition, the temperature class of the contact indicates the maximum temperature it can withstand.

Numerical calculations are required to determine the temperature distribution on each individual contact. However, using specialized software would be a more effective way to calculate temperatures in a relatively short period of time [3,28]. The temperature distribution can be calculated using a variety of programs, one of which is ANSYS, which we used to calculate the temperature distribution.

3.1. High-Current Direct Contact

Electrical contacts that carry high currents are an essential component of many electric devices. The transmission and distribution of electricity is particularly dependent on such devices, and they are subjected to adverse weather conditions which significantly impact their degradation.

The manufacturer of the high-current direct contact we have selected is Ampac (Figure 1). This company produces many contacts with different values of current carrying capacity. The high-current contact we chose for analysis meets all the requirements for optimal power transmission. The elements conducting the electric current are made of copper (main structure) and BeAg (reinforcement plates). The system works without compression springs, which means that its construction is simple and the elementary design of the contact ensures low maintenance costs.

For the analysis, we considered the value of 3000 A, though the given contact can carry up to 4000 A of electric current. The size of the passing electric current depends on the number of contact knives attached to the contact [29].

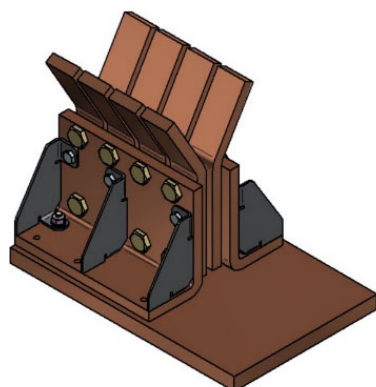


Figure 1. High current direct contact from Ampac [29].

3.2. Direct Contact Parameters

The values given in Table 3 apply to the dimensions shown in the direct contact diagram.

Table 3. Dimensions of individual direct contacts [29].

Current [A]	Dimensions [mm]				Number of Contacts
	B1	B2	L	S	
500 ÷ 1000	50	100	160	10	2
1500	70	120	160	10	4
2000 ÷ 2500	100	150	160	10	6
3000	150	250	160	15	8
4000	200	300	160	20	10

A contact diagram with dimensions is in Figure 2.

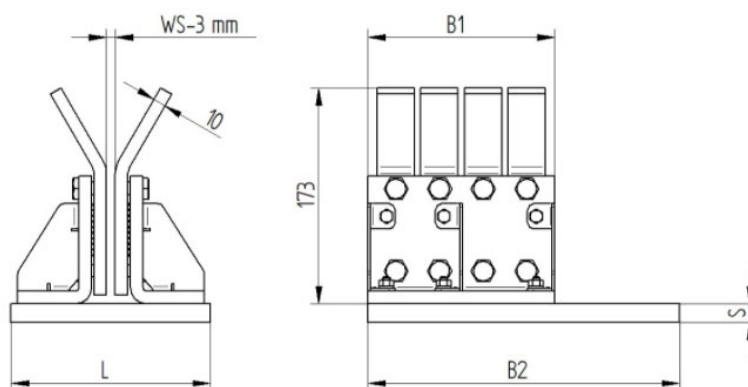


Figure 2. Diagram with dimensions for direct contact [29].

3.3. Simulation of Direct Contact Temperature Distribution

We performed the simulation of the temperature distribution on direct contact using the ANSYS Workbench software. We chose the Workbench version because it allows the creation of object geometry in the 3D interface.

The first step in simulating a contact was to create or select a list of materials, which were later assigned to individual parts. The second step was to create the geometry. A sketch of the contact was created first in 2D resolution, then transformed into a 3D model. After creating all the parts, we set them up as one “Part”, thanks to which the base, the contact holders, the contacts and the contact knife fit together. In the third step, we assigned materials to the individual parts and constructed contact meshing. After that, we determined the boundary conditions of the electric current that began in the base and ended at the knife end.

The last step of the simulation was setting the thermal convection for each part. Based on that, the program displayed the distribution of temperatures at the direct contact point.

In Figure 3, the direct contact with the set values of thermal convections and electric current is visible. Convection (heat flow) is one of the ways of spreading heat in liquids and gases. In ANSYS, however, it represents the so-called heat surface losses. This parameter allows, when modeling, taking into account the way of storing a certain object, such as vertical or horizontal mounting.

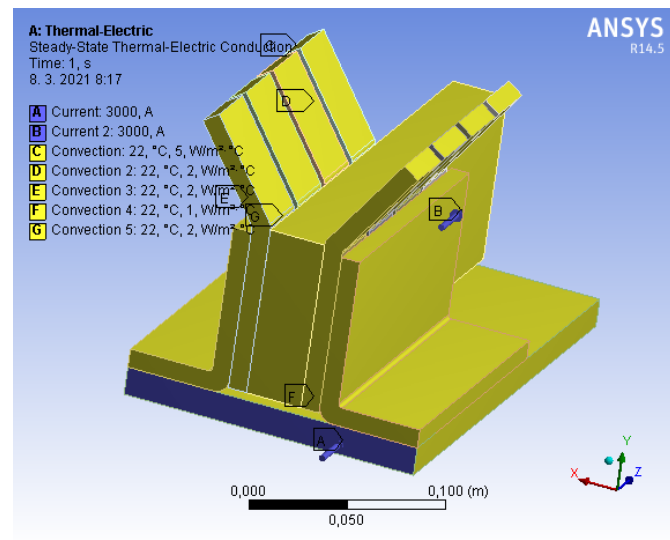


Figure 3. The contact model shows electrical and thermal conditions (points A, B are representing electric current, whereas C–G represent thermal convection).

In our simulation, we considered free thermal convection, which is generated by gravity and has a vertical direction of heat transfer, meaning that heat is dissipated more readily from the upper part of an object than from its sides or lower part [30]. Based on these findings, we set the convection for the upper surfaces of direct contact to $5 \text{ W}/(\text{m}^2 \cdot ^\circ\text{C})$, lateral $2 \text{ W}/(\text{m}^2 \cdot ^\circ\text{C})$ and lower $1 \text{ W}/(\text{m}^2 \cdot ^\circ\text{C})$.

By using higher values, forced thermal convection, which occurs during forced flow, would be considered, e.g., under the influence of a fan. With this type of convection, the direction of heat transfer depends on the direction of airflow.

We neglected the support plates for the contact holders when creating the model, because their main purpose is not to dissipate heat, but to increase mechanical strength.

4. Influence of Materials and Impurities of Direct Contact on Temperature Distribution

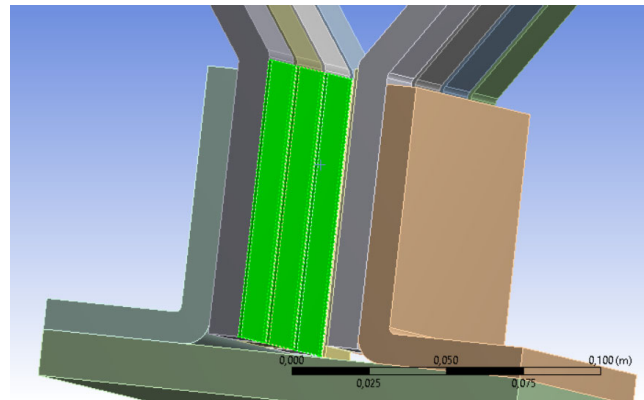
We chose four materials that are often used in electrical engineering in the manufacture of contacts or conductors. The basic material was copper, from which the direct contact is made. Other materials were aluminum, brass and silver, despite the fact that silver is currently used to a lesser extent than the other three materials. We used it because it has better electrical properties than copper [31].

Based on the coefficients of thermal conductivity λ and resistivity ρ , we simulated the effect of different materials on the temperature distribution (on the contact surface). The coefficients of thermal conductivity and resistivity are shown in (Table 4).

Table 4. Material properties of selected individual materials [22].

Material	λ [W/(m·°C)]	ρ [$\Omega\cdot\text{m}$]
Copper	390	1.72×10^{-8}
Aluminum	237	2.65×10^{-8}
Brass	111	6.3×10^{-8}
Silver	428	1.59×10^{-8}
Impurity	30	1×10^{-8} – 1×10^{-4}

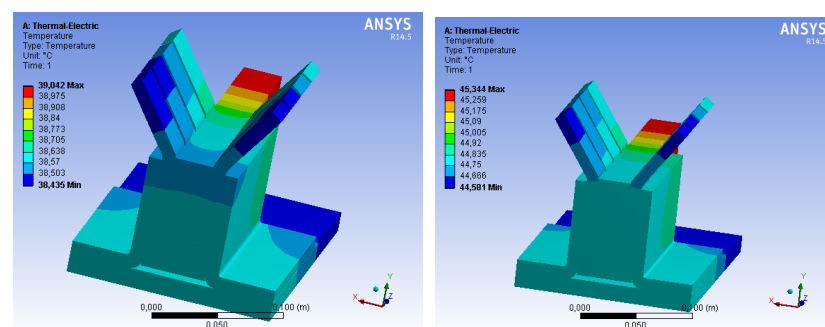
The temperature distribution was studied by adding a volume of 1 mm width to all contact points. As a result of the negative effect of the environment, aging of the material, etc., this volume displays slight wear, unevenness, and particularly oxidation of the contacts. Although impurities of this kind are much thinner, of the order of 10^{-4} mm, due to some imperfections in the program, there is a possibility of errors in the formation of crosslinks on the impurities. These impurities are highlighted in green on Figure 4.

**Figure 4.** An illustrative representation of impurities on contacts (green).

4.1. Influence of Impurities on the Thermal Distribution of Direct Contact from Copper

For our preliminary simulations in the production of a given type of contact, we used copper, as a material used by the manufacturer [29]. On the basis of these simulations, we determined the importance of the input parameters and values, in order to calculate each contact with accuracy.

The temperature distribution in Figure 5 (left) shows that the highest temperature occurred at the beginning of the contact knife, with 39.042 °C being the maximum value. In the middle of the base in the area above the contact holders is the lowest temperature, but also the lowest temperature value reaches 38.435 °C at the ends of the contacts at the end of the knife.

**Figure 5.** Temperature distribution of direct copper contact without impurities (left) and with impurity resistivity of $1 \times 10^{-8} \Omega\cdot\text{m}$ (right).

Contact model (Figure 5, left) was designed without all the mentioned impurities, i.e., it represents the so-called “ideal” operating state, when the contacts do not overheat because of contamination. A higher current value flowing through direct contact could result in overheating in this case. In all other simulations, we used surfaces with impurities. As with materials and impurities, it was necessary to enter the value of the coefficient of thermal conductivity and resistivity. These values are found in Table 4, with the difference that the range of values $1 \times 10^{-8} \div 1 \times 10^{-4} \Omega \cdot \text{m}$.

By creating deteriorating electrical conductivity within this range of resistivity, we produced contamination between the contacts and the contact knife. Small impurities were represented by $1 \times 10^{-8} \Omega \cdot \text{m}$, and very large contamination areas were identified by $1 \times 10^{-4} \Omega \cdot \text{m}$. (Figure 5, right) shows a contact with a resistivity of $1 \times 10^{-8} \Omega \cdot \text{m}$. We presumed this value indicates the actual operating state at the time of initial commissioning.

It is evident from the given temperature distribution that the maximum and minimum values are higher than in the previous state (without impurities), and the temperature increased by around $6 \text{ }^\circ\text{C}$. As in (Figure 5, left), the highest and lowest temperatures occur at the same places, although some of them are slightly higher in the middle of the contact. There is a difference between the ideal and real state of direct contact as reflected in these facts.

Figure 6 represents the state of direct contact, which shows a resistivity of $1 \times 10^{-4} \Omega \cdot \text{m}$ after a long period of use of such a component. Of course, it is impossible to predict that the contact surface may become so dirty after such a period of use. A contaminant, degradation, or damage caused by the same material is not identical among objects made from the same material.

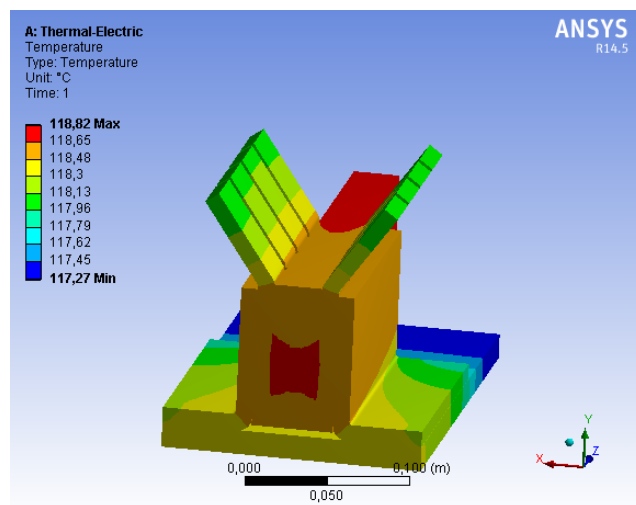


Figure 6. Temperature distribution of direct copper contact and impurity resistivity $1 \times 10^{-4} \Omega \cdot \text{m}$.

In the current example, the maximum temperature is $118.82 \text{ }^\circ\text{C}$, and the minimum is $117.27 \text{ }^\circ\text{C}$. This represents a two-fold increase in temperature compared to the first two cases. Comparing the operating states with the previous “real” and “ideal” states, the “real” operating state had a higher maximum temperature by $73.476 \text{ }^\circ\text{C}$ and the “ideal” operating state had a higher maximum temperature by $79.778 \text{ }^\circ\text{C}$.

Furthermore, there have been significant changes in terms of how each temperature zone is distributed. The so-called warm colors appear to indicate that the areas closest to the knife become the most heated. The temperature of electrical connections can be significantly affected by contamination of the contacts. It is therefore important to clean the contact surfaces regularly in order to ensure that the transmission of energy is as efficient as possible [3,32].

4.2. Summary of the Results of the Temperature Distribution of Direct Contact from Copper

ANSYS is used for the slicing of objects. Using this environment, we place temperature probes at the specific points of the model. These temperature probes allow us to measure the temperature of a discrete element anywhere on the model. Figure 7 illustrates the arrangement of the six probes, which are located in the same locations as the coordinate systems. Just as the name of the temperature probe in the green bubble is written in the picture, so are the others. We entered individual names based on their positions.

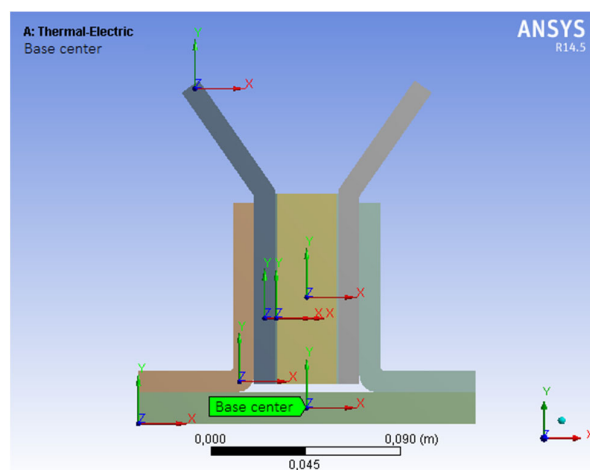


Figure 7. A view of the temperature probes in the middle of the high-current contact.

Tables were created based on temperature values collected from temperature probes. These measured values were used to create graphs showing how temperature changes at various points in the center of contact when various types of impurities are present.

In some cases, the temperature measured by probes, shown in Table 5, is only 0.5 °C differently from the other values. Most of the temperatures occur right in the middle of the knife or impurity. The highest temperature reached was 118.67 °C, and the lowest temperature was recorded at 44.79 °C, which was recorded at the top of the contact.

Table 5. Temperature measurements of the high-current copper contact.

ρ [$\Omega \cdot \text{m}$]	Base Center ϑ [$^{\circ}\text{C}$]	Fold ϑ [$^{\circ}\text{C}$]	Contact Center ϑ [$^{\circ}\text{C}$]	Knife Center ϑ [$^{\circ}\text{C}$]	Impurity Center ϑ [$^{\circ}\text{C}$]	Contact Top ϑ [$^{\circ}\text{C}$]
1×10^{-4}	118.21	118.37	118.62	118.66	118.67	118.11
1×10^{-5}	54.133	54.175	54.236	54.246	54.243	54.066
1×10^{-6}	46.632	46.659	46.696	46.7	46.698	46.564
1×10^{-7}	45.15	45.239	45.272	45.276	45.274	45.147
1×10^{-8}	44.79	44.813	44.845	44.849	44.847	44.723

We placed three curves in two graphs to better show the graphical relationship between them. If six curves were placed in one graph, the characteristics would overlap, and the temperature difference would not be apparent.

Figures 8 and 9 clearly show a non-linear increase in temperature with the increase in impurity resistivity. The temperature increased a small amount along the linear curve for impurities with resistivity values of $10^{-8} \Omega \cdot \text{m}$ and $10^{-6} \Omega \cdot \text{m}$. A significant temperature change occurred from impurity resistivity of $10^{-6} \Omega \cdot \text{m}$ to $10^{-5} \Omega \cdot \text{m}$, with the largest temperature change occurring between $10^{-5} \Omega \cdot \text{m}$ and value $10^{-4} \Omega \cdot \text{m}$.

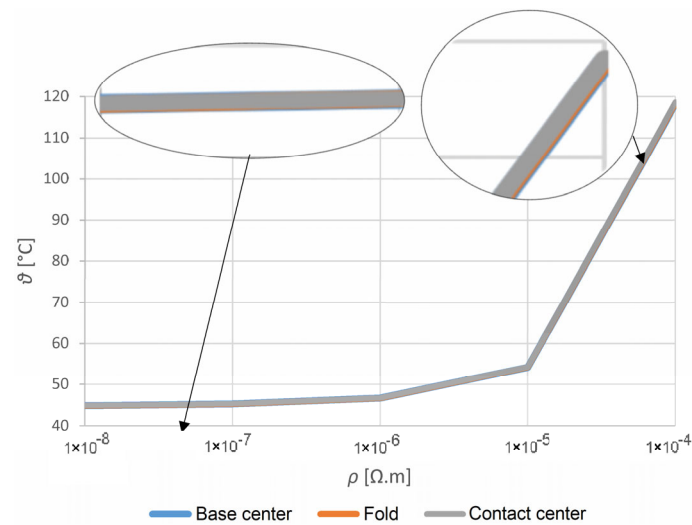


Figure 8. Dependence of impurity resistivity on temperature for high-current copper contacts (for placements: base center, fold, contact center).

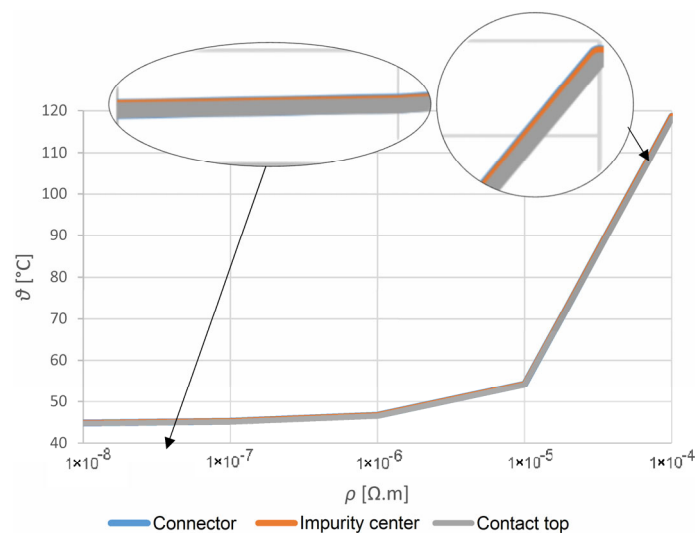


Figure 9. Dependence of impurity resistivity on temperature for high-current copper contacts (for placements: connector, impurity center, and contact top).

In the case of this electric contact, if higher permissible currents are permitted (up to 4000 A), the temperatures obtained will be higher, but still in the allowable range, as stipulated by the electric contact manufacturer [29].

4.3. Comparison of Simulation Results

Graphical dependences on the materials used have so far been described and compared only individually and no temperature differences were clearly visible. Therefore, we extracted only those measurements made at one point (the center of contact) from the tables that contained the measured temperatures, and we then constructed a graphic showing their dependence. We chose this place due to the fact that it is the part of direct contact that was most stressed.

The measured values and the constructed graphical dependence (Figures 10 and 11) showed that the highest temperatures occurred in direct contact from brass and the lowest in direct contact from silver. The temperatures were similarly low for the silver material and the copper material. The symmetry of all nonlinear characteristics of a given dependence

(Figure 11), in which the temperature rises due to increasing contamination of the contacts, is also observable.

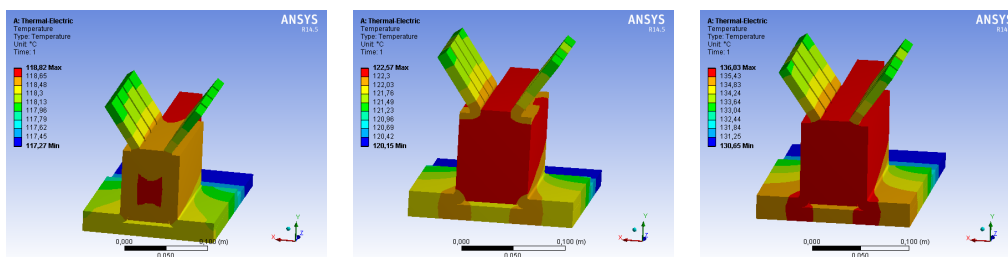


Figure 10. Temperature distribution of direct contact made of copper (left), aluminum (middle) and brass (right) with the highest considered recurrence of impurity $1 \times 10^{-4} \Omega \cdot m$.

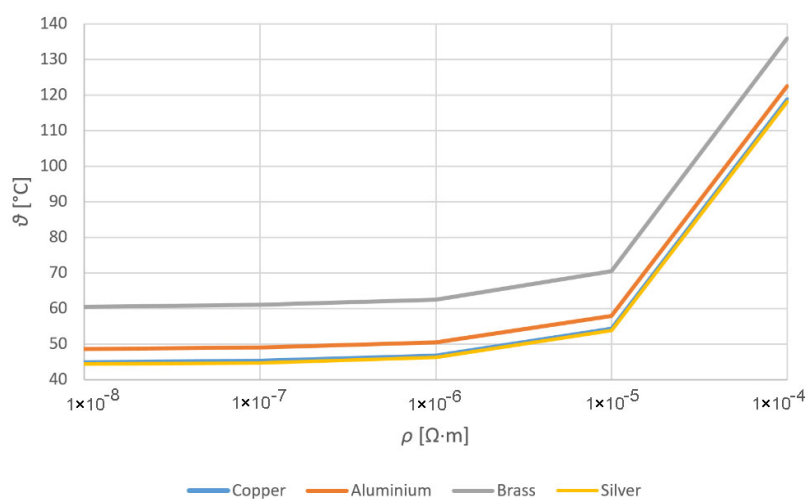


Figure 11. Temperature dependence of impurity resistivity for considered materials in the center of contact.

Based on the simulations, tables, and graphical representations based on them, the copper material selected by the manufacturer for the production of direct contact has the best temperature distribution in comparison with the other materials chosen by us, except for silver. Of course, when choosing a suitable material, manufacturers also take into account their other important properties such as electrical conductivity, mechanical strength, the effect of adverse weather conditions, price and similar matters. It should be summarized that from the point of view of temperature distribution, the most suitable material would be silver, followed by copper, then aluminum and brass.

5. Conclusions

The purpose of this article is to present results of the temperature distribution on the surface of the high current contact, with a nominal current value of 3000 A (there are a range of permissible current values for this type of contact between 500 A and 4000 A). A study of the temperature distribution around a contact point is presented in this paper using ANSYS Workbench. Simulations have shown an increase in temperature with increasing impurity resistivities. Individual degrees of pollutants were represented by individual resistivities, where the largest pollutants corresponded to resistivities with values of $10^{-4} \Omega \cdot m$ and the smallest pollutants to values of $10^{-8} \Omega \cdot m$. By measuring the temperatures at different locations in the middle of the high-current contact, temperature probes also confirmed the rise in temperature. As impurity resistivities increase, we observe a nonlinear increase in temperature. It is crucial to clean the electrical contact surfaces frequently, perform regular inspections, and pay attention to the cleanliness of electrical contacts.

This paper fills the literature gap in the research area related to modeling of high-current contact temperature fields. Moreover, this paper contributes to the communities interested in the thermal processes that want to be more efficient and create new ways to use energy transmission.

Author Contributions: Conceptualization, D.M. and M.P.; methodology, M.K. and L.B.; formal analysis, D.M. and L.B.; simulation validation, D.M. and M.P., experimental validation, L.B. and D.M.; writing—original draft preparation, D.M. and M.P.; writing—review and editing, M.K. and L.B., supervision, M.K.; project administration, D.M.; funding acquisition, M.K. All authors have read and agreed to the published version of the manuscript.

Funding: This work was supported by the Slovak Research and Development Agency under the contract No. APVV-19-0576 and by the Ministry of Education, Science, Research and Sport of the Slovak Republic and the Slovak Academy of Sciences under the contract VEGA 1/0757/21 and VEGA 1/0435/19.

Institutional Review Board Statement: Not applicable.

Informed Consent Statement: Not applicable.

Data Availability Statement: Not applicable.

Conflicts of Interest: The authors declare no conflict of interest. The funders had no role in the design of the study; in the collection, analyses, or interpretation of data; in the writing of the manuscript, or in the decision to publish the results.

References

1. IEEE Standard Dictionary of Electrical and Electronics Terms. In *IEEE Transactions on Power Apparatus and Systems*; IEEE: Piscataway, NJ, USA, 1980; Volume PAS-99, p. 37a. [\[CrossRef\]](#)
2. Grachev, N.; Andryukhin, A.; Chernoverskaya, V. Investigation of the Characteristics of the Transient Electrical Resistance of Contacts in the Designs of Radio Electronic Devices in the Conditions of the Formation of Contact Radio Interference. In Proceedings of the 2021 International Seminar on Electron Devices Design and Production (SED), Prague, Czech Republic, 27–28 April 2021; pp. 1–5. [\[CrossRef\]](#)
3. Medved, D.; Presada, J. Thermal Analysis of High-current Electric Contact. *Acta Electrotech. Inform.* **2021**, *21*, 38–42. [\[CrossRef\]](#)
4. Medved, D.; Zbojovský, J. Influence of the Position of the Electrical Contact on the Size of the Temperature Distribution. *Prz. Elektrotech.* **2021**, *97*, 230–233. [\[CrossRef\]](#)
5. Gatzsche, M.; Lücke, N.; Großmann, S.; Kufner, T.; Freudiger, G. Validity of the voltage-temperature relation for contact elements in high power applications. In Proceedings of the IEEE 61st Holm Conference on Electrical Contacts (Holm), San Diego, CA, USA, 11–14 October 2015; pp. 29–38. [\[CrossRef\]](#)
6. Behrens, V.; Siegle, E.; Schreiber, J.; Honig, T.; Finkbeiner, M. Effect of Ambient Temperature and Contact Force on Contact Resistance and Overtemperature Behaviour for Power Engineering Contacts. In Proceedings of the IEEE 58th Holm Conference on Electrical Contacts (Holm), Portland, OR, USA, 23–26 September 2012; pp. 1–6. [\[CrossRef\]](#)
7. Israel, T.; Gatzsche, M.; Schlegel, S.; Großmann, S.; Kufner, T.; Freudiger, G. The impact of short circuits on contact elements in high power applications. In Proceedings of the IEEE Holm Conference on Electrical Contacts, Denver, CO, USA, 10–13 September 2017; pp. 40–49. [\[CrossRef\]](#)
8. Paunescu, M.; Dan, M.; Dragan, F.; Topa, V. The Effect of Corrosion on Electrical Contacts. In Proceedings of the 8th International Conference on Modern Power Systems (MPS), Cluj-Napoca, Romania, 21–23 May 2019; pp. 1–4. [\[CrossRef\]](#)
9. Damle, T.; Xu, C.; Varenberg, M.; Graber, L. Electric Field Between Contacts of Fast Mechanical Switches Subjected to Fretting Wear. In Proceedings of the IEEE 66th Holm Conference on Electrical Contacts and Intensive Course (HLM), San Antonio, TX, USA, 30 September–7 October 2020; pp. 144–148. [\[CrossRef\]](#)
10. Shen, Q.; Lv, K.; Liu, G.; Qiu, J. Impact of Electrical Contact Resistance on the High-Speed Transmission and On-Line Diagnosis of Electrical Connector Intermittent Faults. *IEEE Access* **2017**, *5*, 4221–4232. [\[CrossRef\]](#)
11. Byerly, J.M.; Schneider, C.; Schloss, R.; West, I. Real-time circuit breaker health diagnostics. In Proceedings of the 70th Annual Conference for Protective Relay Engineers (CPRE), College Station, TX, USA, 3–6 April 2017; pp. 1–6. [\[CrossRef\]](#)
12. Carvou, E.; Ben Jemaa, N.; Porte, M.; Razafiarivelo, J. Contact heating by long arcing during connector disconnection. In Proceedings of the Fifty-First IEEE Holm Conference on Electrical Contacts, Chicago, IL, USA, 26–28 September 2005; pp. 360–365. [\[CrossRef\]](#)
13. Parkansky, N.; Boxman, R.L.; Goldsmith, S.; Rosenberg, Y. Arc erosion reduction on electrical contacts using transverse current injection. *IEEE Trans. Plasma Sci.* **1997**, *25*, 543–547. [\[CrossRef\]](#)
14. Zhou, Y.; Lv, Y.; Wang, H.; Ma, A.; Liu, H. Electrical Contact Behavior of Several Typical Materials in Dust at Static and Dynamic Conditions. In Proceedings of the 56th IEEE Holm Conference on Electrical Contacts, Charleston, SC, USA, 4–7 October 2010; pp. 1–12. [\[CrossRef\]](#)

15. Xixiu, W.; Meihua, D.; Zhenbiao, L.; Chengyan, L. The composition change of contact material surface. In Proceedings of the Forty-Ninth IEEE Holm Conference on Electrical Contacts, Washington, DC, USA, 10 September 2003; pp. 139–144. [CrossRef]
16. Saha, S.; Wynne, S.; Jackson, R.L. Electro-thermo-mechanical Contact Analysis Considering Temperature Dependent Material Properties and Electrical Contact Resistance Determination. In Proceedings of the IEEE 66th Holm Conference on Electrical Contacts (HLM), San Antonio, TX, USA, 24–27 October 2021; pp. 8–15. [CrossRef]
17. Monnier, A.; Froidurot, B.; Jarrige, C.; Meyer, R.; Teste, P. A mechanical, electrical, thermal coupled-field simulation of a sphere-plane electrical contact. In Proceedings of the Fifty-First IEEE Holm Conference on Electrical Contacts, Chicago, IL, USA, 26–28 September 2005; pp. 224–231. [CrossRef]
18. Szulborski, M.; Łapczyński, S.; Kolimas, L.; Zalewski, D. Transient Thermal Analysis of the Circuit Breaker Current Path with the Use of FEA Simulation. *Energies* **2021**, *14*, 2359. [CrossRef]
19. Vinaricky, E. *Elektrische Kontakte, Werkstoffe und Anwendungen*; Springer: Berlin/Heidelberg, Germany, 2016. [CrossRef]
20. Elbekri, T.; Chaâbane, L. Experimental investigation on parameters of switches contacts. In Proceedings of the 26th International Conference on Electrical Contacts (ICEC 2012), Beijing, China, 14–17 May 2012; pp. 390–392. [CrossRef]
21. Kubler-Riedinger, M.; Bauchire, J.-M.; Hong, D.; Déplaudé, G.; Joyeux, P. Electrical and Morphological Investigations of Electrical Contacts used in Low-Voltage Circuit-Breakers. In Proceedings of the IEEE 66th Holm Conference on Electrical Contacts and Intensive Course (HLM), San Antonio, TX, USA, 30 September–7 October 2020; pp. 115–122. [CrossRef]
22. Chen, J.; Yang, F.; Luo, K.; Wu, Y.; Rong, M. Experimental investigation of the electrical contact characteristics in Rolling Contact Connector. In Proceedings of the IEEE 61st Holm Conference on Electrical Contacts (Holm), San Diego, CA, USA, 11–14 October 2015; pp. 235–240. [CrossRef]
23. Dyck, T.; Bund, A. Design of Contact Systems Under Consideration of Electrical and Tribological Properties. *IEEE Trans. Compon. Packag. Manuf. Technol.* **2018**, *8*, 427–438. [CrossRef]
24. Zhou, X.; Schoepf, T. Characteristics of Overheated Electrical Joints Due to Loose Connection. In Proceedings of the IEEE 57th Holm Conference on Electrical Contacts (Holm), Minneapolis, MN, USA, 11–14 September 2011; pp. 1–7. [CrossRef]
25. Tang, L.; Ruan, J.; Yang, Z.; Chen, R.; Li, G.; Yin, X. Hotspot Temperature Monitoring of Fully Insulated Busbar Taped Joint. *IEEE Access* **2019**, *7*, 66463–66475. [CrossRef]
26. Obach, I.I.; Abouellail, A.A.; Soldatov, A.I.; Soldatov, A.A.; Sorokin, P.V.; Shinyakov, Y.A.; Sukhorukov, M.P. Monitoring of Power Supply. In Proceedings of the International Siberian Conference on Control and Communications (SIBCON), Tomsk, Russia, 18–20 April 2019; pp. 1–6. [CrossRef]
27. Cesky, L.; Janicek, F.; Kubica, J.; Skudrik, F. Overheating of primary and secondary coils of voltage instrument transformers. In Proceedings of the 18th International Scientific Conference on Electric Power Engineering (EPE), Kouty nad Desnou, Czech Republic, 17–19 May 2017; pp. 1–6. [CrossRef]
28. Rot, D.; Kozeny, J.; Jirinec, S.; Jirinec, J.; Podhrazky, A.; Poznyak, I. Induction melting of aluminium oxide in the cold crucible. In Proceedings of the 18th International Scientific Conference on Electric Power Engineering (EPE), Kouty nad Desnou, Czech Republic, 17–19 May 2017; pp. 1–4. [CrossRef]
29. Ampac. High Current Direct-Contacts 500 up to 4000 Ampere. Available online: <https://www.ampacremscheid.de/en/products/high-current-contacting-for-galvano-and-eloxal-technology/direct-contacts/> (accessed on 8 September 2021).
30. Wang, Y. Coupled Electromagnetic and Thermal Analysis and Design Optimization of Synchronous Electric Machines. Master's Thesis, University of Wisconsin-Milwaukee, Milwaukee, WI, USA, 2014.
31. Ekpu, M.; Bhatti, R.; Ekere, N.; Mallik, S. Advanced thermal management materials for heat sinks used in microelectronics. In Proceedings of the 18th European Microelectronics & Packaging Conference, Brighton, UK, 12–15 September 2011; pp. 1–8.
32. Chudnovsky, B.H. Electrical Contacts Condition Diagnostics Based on Wireless Temperature Monitoring of Energized Equipment, Electrical Contacts–2006. In Proceedings of the 52nd IEEE Holm Conference on Electrical Contacts, Montreal, QC, Canada, 25–27 September 2006; pp. 73–80. [CrossRef]